Evidence for a Continuous Transition from Nonadiabatic to Adiabatic Proton Transfer Dynamics in Protic Liquids

Boiko Cohen and Dan Huppert*

Raymond and Beverly Sackler Faculty of Exact Sciences, School of Chemistry, Tel Aviv University, Tel Aviv 69978, Israel

Received: August 18, 2000; In Final Form: December 7, 2000

The reversible proton dissociation and geminate recombination of photoacids is studied as a function of temperature in monols, diols, and glycerol. For this purpose, we use a strong photoacid 5,8-dicyano-2-naphthol (DCN2) ($pK_a^* \approx -4.5$ in water), capable of transferring a proton to alcohols. The experimental data are analyzed by the Debye−Smoluchowski equation, which is solved numerically with boundary conditions to account for the reversibility of the reaction. At high temperature, the proton-transfer rate is almost temperature independent, whereas at low temperature, the rate constant has strong temperature dependence. The unusual temperature dependence is explained using Borgis−Hynes proton transfer theory, based on the Landau−Zener curve crossing formulation. The high-temperature behavior of the rate constant denotes the nonadiabatic limit, whereas the low-temperature behavior denotes the adiabatic limit. We have used an approximate expression for the proton-transfer rate, which bridges the nonadiabatic and the solvent controlled adiabatic limit to fit the temperature dependence curve of the experimental proton-transfer rate constant.

Introduction

The study of Excited-State Proton Transfer (ESPT) reactions in solution is fundamental to the understanding of the nature of the reactions of acids and bases in solution. These studies were conducted on a photoacid molecule that dissociates upon excitation to produce an excited anion and a proton.[1−4] Even though this subject has been studied for more than forty years,[5,6] the exact nature of ESPT reactions is still not completely clear, and neither is the dual role played by the solvent molecule (1) as proton acceptor and (2) as a solvating medium of both the reactant and the product.[7−9]

A large effort in the past four decades has been made to understand the dynamics of proton transfer in the gas phase, in clusters, and in the condensed phase.[10−13]

The fundamental theoretical framework for the analysis of kinetics for proton/deuteron transfer is the transition-state theory.[14−17] In this theory, a classical transition state is defined by the free-energy maximum along the reaction coordinate. Isotope effects are calculated in terms of the difference between the zero-point energies for the transition state and the reactant. An additional effect of proton or deuteron tunneling through the barrier is expected to enhance the isotope effect. Approximate theories about proton tunneling in chemistry are based on the work of Bell.[15,17] The evidences of tunneling are taken to be a large kinetic isotope effect (KIE) and concave curved Arrhenius plots of k vs $1/T$, i.e., at low temperatures the proton/deuteron transfer rate constant exhibits a lower temperature dependence.

More recent theories have revealed that tunneling is the dominant reaction mode for proton transfer, even at ambient temperatures. The theoretical development for solution-phase proton-transfer reaction has been undertaken by Dogonadze, Kuznetzov, Ulstrup, and co-workers[18] and then extended by Borgis and Hynes, Cukier, and Voth.[19−21] These theories suggest that when a potential energy barrier is present in the proton-reaction coordinate, the reaction pathway involves tunneling through the barrier, as opposed to passage over barrier.

In a recent paper,[22] we described our experimental results on an unusual temperature dependence of excited-state proton transfer from a super photoacid (5,8 dicyano-2-naphthol, DCN2) to methanol, ethanol, and propanol. At temperatures above 285 K the rate of the proton transfer in methanol is almost temperature independent, whereas at $T < 250$ K, the rate exhibits large temperature dependence. The rate constant is similar to the inverse of the dielectric relaxation time. We proposed a simple stepwise model to describe and calculate the temperature dependence of the proton transfer to the solvent reaction. The model accounts for the large difference in the temperature dependence and the proton-transfer rate at high and low temperatures.

In the following paper, we extended the measurements of the dynamics of excited-state intermolecular proton transfer (ESPIT) from DCN2 to a large number of monols, diols, and glycerol as a function of temperature. The temperature dependence of the rate constant for proton transfer in these solvents is explained as a continuous transition from nonadiabatic (high temperature) to adiabatic (low temperature) proton transfer to the solvent. This phenomenon can be understood by the Landau−Zener curve-crossing formulation developed for proton-transfer rate constant by Borgis and Hynes.[19]

Experimental Section

Time-resolved fluorescence was measured using the time-correlated single-photon counting (TCSPC) technique. As an excitation source, we used a cw mode-locked Nd:YAG-pumped dye laser (Coherent Nd:YAG Antares and a 702 dye laser), providing a high repetition rate (>1 MHz) of short pulses (2 ps at full width half-maximum, fwhm). The (TCSPC) detection

* To whom correspondence should be addressed. E-mail: huppert@chemosf1.tau.ac.il. Fax/Phone: 972-3-6407012

10.1021/jp002979g CCC: $20.00
Published on Web 03/02/2001

system is based on a Hamamatsu 3809U, photomultiplier, Tennelec 864 TAC, Tennelec 454 discriminator, and a personal computer-based multichannel analyzer (nucleus PCA-II). The overall instrumental response was about 50 ps (fwhm). Measurements were taken at 10 nm spectral width. Steady-state fluorescence spectra were taken using a SLM AMINCO−Bowman-2 spectrofluoremeter.

DCN2 was synthesized by Tolbert and co-workers.[23] The sample concentrations were between 2×10^{-4} and 2×10^{-5} M. Solvents were reagent grade and were used without further purification. The solution's pH was about 6.

The DCN2 fluorescence spectrum consists of two structureless broad bands (∼40 nm fwhm). The emission band maximum of the acidic form (ROH*) emits at 450 nm in water and in alcohols. The emission band maximum of the alkaline form (RO^-*) emits at 600 nm in water and in alcohols. At 450 nm, the overlap of the two luminescence bands is rather small and the contribution of the RO^-* band to the total intensity at 450 nm is about 0.5%. In addition, we find that some fluorescent impurity in the DCN2 compound increases the fluorescence intensity at long times to a level of 2% of the peak intensity. Therefore, in the time-resolved analysis we add to the calculated signal an additional exponential decay of 10 ns with amplitude of about 2% to compensate for the impurity fluorescence. To avoid ambiguity due to overlap between fluorescence contributions of ROH* and RO^-*, we mainly monitored the ROH* fluorescence at 450 nm.

The temperature of the irradiated sample was controlled by placing the sample in an oven or a liquid N_2 cryostat with thermal stability of approximately ± 1K.

Results and Discussion

A. Proton Dissociation and Geminate Recombination in the Liquid Phase. *1. General Considerations.* Experimental and theoretical studies of ESPT processes in solution have led to the development of a two step model[24,25] (Scheme 1).

SCHEME 1

$$ROH^* \underset{k_r}{\overset{k_d}{\rightleftharpoons}} [RO^-{}^*...H^+]_{(r=a)} \overset{DSE}{\rightleftharpoons} RO^-{}^* + H^+$$

The first step is described by back-reaction boundary conditions with intrinsic rate constants k_d and k_r. This is followed by a diffusional second step in which the hydrated proton is removed from the parent molecule. This latter step is described by the Debye−Smoluchowski equation (DSE). In the continuous diffusion approach, one describes the photoacid dissociation reaction by the spherically symmetric diffusion equation (DSE)[26] in three dimensions.[24,25] The boundary conditions at $r = a$ are those of back reaction, (Scheme 1). k_d and k_r are the "intrinsic" dissociation and recombination rate constants at the contact sphere radius a. Quantitative agreement was obtained between theory and experiment[24,25] and, as a result, it was possible to make a closer study of the ESPT process itself, as well as the dynamic and static properties of the solvent.

An important parameter in our model is the mutual diffusion coefficient $D = D_{H^+} + D_{RO^-}$. The temperature dependence of the proton diffusion constant, D_{H^+}, for various alcohols was deduced from the proton conductance measurements as a function of T.[27,28] The anion diffusion constant, D_{RO^-}, as a function of T was estimated from the solvent viscosity data.[29] The temperature dependence of the dielectric constant and the dielectric relaxation of neat alcohols data was taken from Refs 30−33. Figure 1 shows, on a semilog scale, the time-resolved

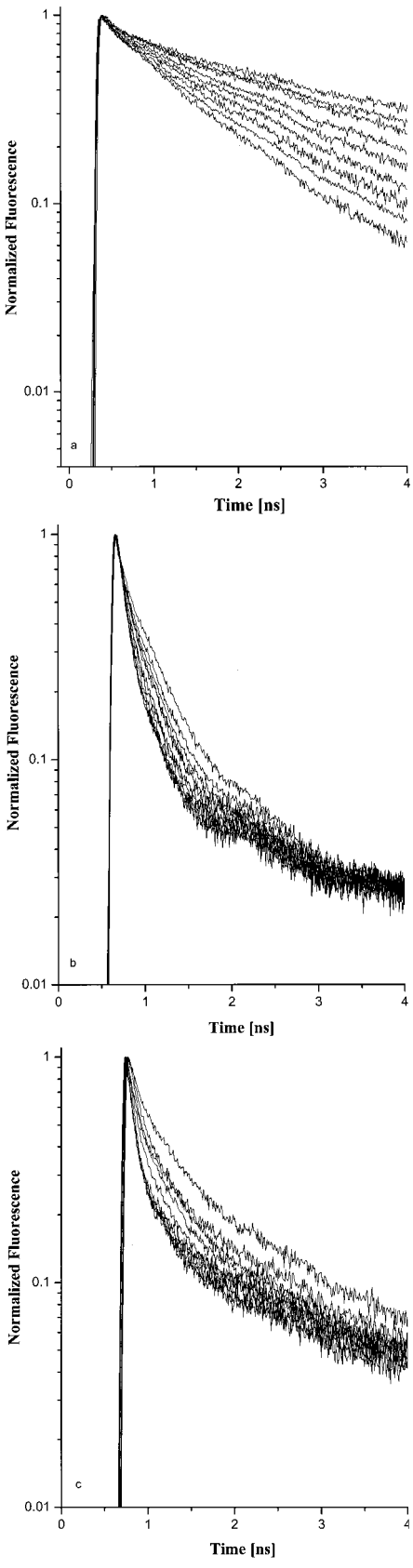

Figure 1. (a) Time-resolved emission of DCN2 in glycerol solution of the protonated form (ROH*) measured at several temperatures in the range 295−410 K. (b) Time-resolved emission of DCN2 in ethylene glycol solution of the protonated form (ROH*) measured at several temperatures in the range 295−373 K. (c) Time-resolved emission of DCN2 in 1,4-butanediol solution of the protonated form (ROH*) measured at several temperatures in the range 295−393 K.

emission intensity of DCN2 in ethanediol (1a), 1,4-butanediol (1b) and glycerol (1c) solutions measured at 450 nm at various temperatures in the range of 273−415 K. Using Scheme 1 and the numerical solution of the DSE,[24] we fitted the experimental data and extracted both the intrinsic proton dissociation and recombination (k_d and k_r) rate constants. Typical chi-squares of the fit range from 1.2 to 2. We determined the proton-transfer rate constant, k_d, from the fit to the initial fast decay of the ROH* fluorescence (∼150 ps for DCN2 in glycerol at 400 K). The initial fast component of the fluorescence decay is mainly determined by the deprotonation process and is almost insensitive to the geminate recombination process. The long time behavior (the fluorescence tail) seen in the ROH* time-resolved emission is a consequence of the repopulation of the ROH* species by reversible recombination of RO^-* with the geminate proton. The reprotonation is an adiabatic process, and therefore, the excited ROH* can undergo a second cycle of deprotonation. The overall effect is a nonexponential fluorescence tail.[24]

The comparison of the numerical solution with the experiment involves several parameters. Some are adjustable parameters, like k_d and k_r, others, like the contact radius, a, have acceptable literature values.[24,25] The static dielectric constant, ϵ, is known as a function of the temperature for the solvents used. There may be uncertainties concerning the values of the mutual diffusion constant, D, at low temperatures. Thus, we are facing a multiparameter problem in adjusting a solution of a partial differential equation to fit the experimental data.

The asymptotic expression (the long time behavior) for the fluorescence of ROH*(t) is given by[34]

$$[\mathrm{ROH}^*] \cong \frac{\pi}{2} a^2 \exp(R_D/a) \frac{k_r}{k_d(\pi D)^{3/2}} t^{-3/2} \qquad (1)$$

In the above equation, R_D is the Debye Radius, given by

$$R_D = \frac{|z_1||z_2|e^2}{\epsilon k_B T} \qquad (2)$$

where z_1 and z_2 are the charges of the proton and anion, ϵ is the static dielectric constant of the solvent, and the absolute temperature T. The variable e is the electronic charge, and k_B is Boltzmann's constant. Equation 1 shows that uncertainty in the determination of $D(T)$ causes a larger uncertainty in k_r. Also, the relatively large fluorescence "background", due to fluorescent impurity in the DCN2 compound, prevents us to determine accurately the recombination rate constant. We estimate that the error in determination of k_d is 5%. The error in the determination of k_d is due to (1) the signal-to-noise ratio of the experimental signal, which affects the fluorescence curve at longer times and (2) the interplay between k_d and k_r (see eq 1) at longer times. The uncertainty in the determination of k_r is estimated to be much larger, ∼20%. The relatively large uncertainty in the values of k_r arises from the complex relation between the above-mentioned parameters, which determine the ROH* fluorescence tail and the large background due to fluorescence of impurity in the DCN2 sample.

B. Temperature Dependence of the Proton-Transfer Rate. A semilog plot of the dissociation rate constant, k_d, of DCN2 in methanol, ethanol propanol, ethanediol, 1,4 -butanediol, and glycerol solutions versus $1/T$ is shown in Figure 2a. The variable k_d in methanol and ethanol is almost independent of the liquid temperature (in the range +60 °C to +20 °C). The temperature dependence of k_d in propanol at the high-temperature range is larger than that in methanol and ethanol. At lower temperatures,

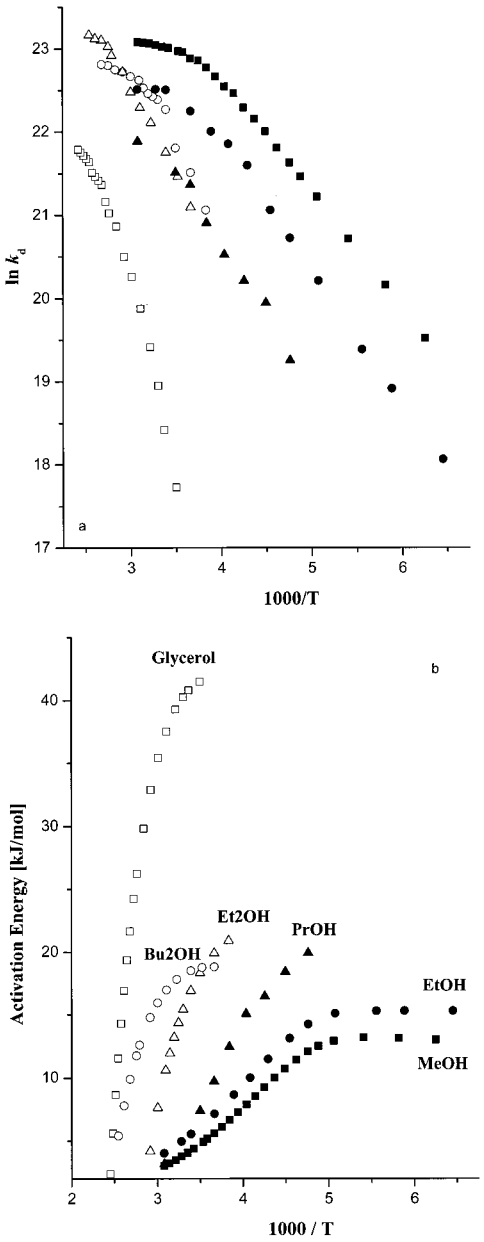

Figure 2. (a) Arrhenius plot of the proton-transfer rate constant of DCN2 in methanol (■), ethanol (●), propanol (▲), 1,4-butanediol (○), ethylene glycol (Δ), and glycerol (□) as a function of $1/T$. (b) The activation energies of the proton-transfer rate in methanol (■), ethanol (●), propanol (▲), 1,4-butanediol (○), ethylene glycol (Δ), and glycerol (□) as a function of *1/T*.

k_d in all the alcohols used in this study decreases rapidly as the temperature decreases.

The temperature dependence of k_d is quite unusual for chemical reactions. In general, chemical reactions obey a constant exponential (Arrhenius) decrease of the reaction rate constant as a function of $1/T$ in a large temperature range. As described before, the value of k_d is almost insensitive to the solvent temperature at $T > 10$ °C whereas, below −20 °C, k_d decreases with the decrease in the sample temperature with a relatively large activation energy.

The activation energies of k_d of DCN2 in the liquid phase of the above-mentioned solutions as a function of $1/T$ are shown in Figure 2b. The activation energies are obtained by differentiating a polynomial fit of the data in Figure 2a. At the low-temperature range, < 10 °C, the activation energy of k_d in all the monols increases monotonically as T decreases and

approaches a constant value similar to the one of the dielectric relaxation time. The literature values[30] of the activation energies of τ_D are 12, 16, 21, and 48 kJ/mol for methanol, ethanol, propanol, and glycerol, respectively. For the proton-transfer activation energies at low temperatures, we obtained 13, 15.5, and 20 kJ/mol for methanol, ethanol, and propanol, respectively.

Discussion

In the following section, we first present theoretical developments related to nonadiabatic and adiabatic proton transfers. This will then be followed by a description of our previous model accounting for the temperature dependence of proton-transfer rate. Finally, a correlation of our model of proton transfer with the theory will be presented.

The model for nonadiabatic proton-transfer developed by Kuznetsov and his colleagues[18] is very similar to the model for nonadiabatic electron transfer in its treatment of the involvement of solvent. The fundamental assumption is that when a barrier is encountered in the proton transfer coordinate, the proton tunnels through the barrier, thus leading to a nonadiabatic process. This assumption is fundamentally different from the Bell[15] picture, where proton tunneling occurs only in the region at the top of the reaction barrier. In the Kuznetsov model,[18] when the polar solvent is equilibrated to the reactant, the proton will not be transferred due to an energy mismatch in the reactant and product states. Upon a solvent fluctuation, the energy of the reactant and product states becomes equal, and it is in this solvent configuration that the proton tunnels from one side of the well to the other. Finally, upon solvent relaxation, the product state is formed.

If the pretunneling and post-tunneling configurations are regarded as real, transient intermediates, the process can be described by a set of chemical equations[35]

$$AH + S_B + S_R \underset{k_{-1}}{\overset{k_1}{\rightleftharpoons}} AH{\cdot}S_B + S_{\neq}$$

$$AH{\cdot}S_B + S_{\neq} \underset{k_{-2}}{\overset{k_2}{\rightleftharpoons}} A^-{\cdot}HS_B + S_{\neq}$$

$$A^- + HS_B + S_{\neq} \xrightarrow{k_3} A^- + HS_B + S_p$$

where AH is the protonated photoacid, S_B is a single solvent molecule to which the proton is transferred, S_R is the solvent configuration to stabilize the reactants, and S_p is the solvent configuration of the products. $S_{\neq}$ is the solvent configuration to equally stabilize $AH{\cdots}S_B$ and $A^-{\cdots}HS_B$.

The initial ideas put forth by Dogonadze, Kuznetzov, Ulstrup, and co-workers[18] for nonadiabatic proton transfer were extended by Borgis and Hynes.[19] They addressed the important issue of low frequency vibrations in promoting proton transfer. One important difference between electron transfer and proton transfer is the extreme sensitivity of the proton tunneling matrix element to distance. The functional form of the tunneling coupling matrix element between the reactant and product state, for moderate to weakly coupling, is $c(Q) = C_0 \exp(-\alpha\delta Q)$. The decay parameter α is very large, 25−35 $Å^{-1}$, when compared to the corresponding decay parameter for the electronic coupling in electron transfer, 1 $Å^{-1}$. It is this feature that makes the dynamics of proton transfer so sensitive to the internuclear separation of the two heavy atoms. Although a decrease of 0.2 Å will increase the rate of electron transfer only by a factor 1.21, a similar distance change in proton transfer will increase the rate by a factor of ∼400.

The Borgis−Hynes[19] model introduces a low-frequency vibrational mode, Q, whose frequency is ω_Q, and the associated vibrational reorganization energy is E_Q. They derived the nonadiabatic rate constant, k. It was similar to that of Kuznetsov and co-workers[18] but the tunneling term is significantly modified. The tunneling term strongly depends on a promoting vibration, Q, and the proton-transfer rate increases with respect to the Kuznetsov fixed equilibrium distance formula.

A simpler model was used by Bernstein and co-workers to calculate the proton-tunneling rate in gas-phase van der Waals clusters.[11] The model employed consists of three essential features: (1) the untransferred and transferred structures are separated from one another by a potential-energy barrier that can be characterized by a width and height, (2) the barrier width and height are modulated by vibrational excitation of the intermolecular cluster modes, and (3) vibrational energy is distributed statistically among the vibrational (van der Waals) modes. Tunneling rates can be calculated as a function of the heavy atom separation based upon the WKB approximation for particle penetration through a barrier of assumed functional form.

The barrier height and width are modulated by the stretching mode between the photoacid and the accepting solvent molecule near the OH group of the donor. Calculations of the proton-transfer rate of this simple model reveal that the stretching mode has a profound effect on the proton-transfer rate. For a parabolic barrier shape and a barrier height of 8000 cm^{-1} and half width of 0.2 Å, and intermolecular vibrational frequency of ∼120 cm^{-1}, the tunneling rate increases by more than 3 orders of magnitude from 10^8 s^{-1} to 10^{11} s^{-1}.

A. Qualitative Model for the Temperature Dependence of Excited-State Proton-Transfer Reactions. The main findings of the experiments are as follows:

1. DCN2 transfers a proton in the excited state to protic solvents.

2. At relatively low temperature, the temperature dependence of the ESPIT rate constant follows $1/\tau_D$, where τ_D is the slow component of the dielectric relaxation.

3. In contrast to the low temperature behavior, at relatively high temperatures, the proton-transfer rate constant is almost temperature independent.

4. Similarly, we find high-temperature asymptotic behavior on a much limited temperature range for other photoacids like HPTS and other naphthol derivatives in water.[36]

Previous Model of Proton-Transfer Rate Constant. Previously, we used a qualitative model that accounts for the unusual temperature dependence of the excited-state proton transfer. The proton-transfer reaction depends on two coordinates; the first one depends on a generalized solvent configuration. For the alcohols used in this study, the solvent coordinate characteristic time is within the range of the dielectric relaxation time τ_D and the longitudinal relaxation $\tau_L = (\epsilon_0)/(\epsilon_s)\tau_D$. The second coordinate is the actual proton translational motion (tunneling) along the reaction path.

The model restricts the proton transfer process to be stepwise. The proton moves to the adjacent hydrogen bonded solvent molecule only when the solvent configuration brings the system to the crossing point according to Kuznetsov model.[18] This simple model excludes parallel routes for the ESPT in which many solvent configurations permit the reaction to take place with a distribution of reaction rates, whereas in a two-dimensional model, these parallel routes are permitted and contribute to the overall effective rate. In the stepwise model, the overall proton-transfer time is a sum of two times, $\tau = \tau_1$

$+ \tau_2$, where τ_1 is the characteristic time for the solvent reorganization, and τ_2 is the time for the proton to pass to the acceptor. The overall rate constant, $k_d(T)$, at a given T is

$$k_d(T) = \frac{k_H(T)k_S(T)}{k_H(T) + k_S(T)} \tag{3}$$

where k_S is the solvent coordinate rate constant, and k_H is the proton coordinate rate constant.

Equation 3 provides the overall excited-state proton-transfer rate constant along the lines of a stepwise process similar to the processes mentioned above. As a solvent coordinate rate constant, we use $k_S(T) = b/\tau_D$, where b is an adjustable empirical factor determined from the computer fit of the experimental data. We find that the empirical factor lies between 0.65 and 4. For the alcohols, τ_L is usually smaller than τ_D by a factor of 2−6. Thus, the solvent characteristic time, $\tau_S = 1/k_S(T)$, for monols lies between the dielectric relaxation and the longitudinal time, $\tau_L < \tau_S < \tau_D$. The reaction rate constant, k_H, along the proton coordinate is expressed by the usual activated chemical reaction description given by eq 4. At high temperatures, the solvent relaxation is fast and the rate determing step is the actual proton-transfer coordinate.

$$k_H = k_H^0 \exp\left(-\frac{\Delta G^{\neq}}{RT}\right) \tag{4}$$

where k_H^0 is the preexponential factor determined by the fit to the experimental results and $\Delta G^{\neq}$ is the activation energy.

The activation energy, $\Delta G^{\neq}$, is determined from the excited-state acid equilibrium constant, K_a^*, and the structure reactivity relation of Agmon and Levin.[37] K_a^* is calculated from the rate parameters derived from the time-resolved emission at ∼320 K, assuming that $k_H \simeq k_d$ according to

$$K^*_{a,chem} = 10^{27} k_d/(N_A k_a) \tag{5}$$

where N_A is Avogadro's number and $k_a = 4\pi a^2 k_r$.[22]

Temperature Dependence and the Free Energy Relationship. Pines and co-workers[38] correlated the value of the proton dissociation rate k_d of many photoacids with their pK_a^* value. They used the structure reactivity relation published by Agmon and Levine.[37] Recently, Solntsev et al.[39] used the same type of free energy correlation for 5-cyano-2-naphthol in several solvents. The basic assumption in such a correlation is that, within a family of similar reactions, the intrinsic free-energy barrier for the reaction is modified by the total free energy change following the reaction. When the reaction is endothermic, $\Delta G \gg 0$, such correlation predicts a slope of one between ln$k$ and ΔG. This correlation predicts asymptotic behavior at $\Delta G \ll 0$, $\Delta G^{\neq} = 0$ (i.e., a slope of zero in the correlation of ln$k$ and ΔG) and that the reaction rate constant will assume the value of the preexponential factor. Marcus's theory, as well as Kuznetsov's theory, predicts that when $\Delta G \ll 0$ the reaction rate constant decreases (the inverted region). Pines et al.[38] found that the plot of ln$k$ versus ΔG of photoacids behaves as predicted by the Agmon and Levine theory.[37] At the limit of large exothermicity, $\Delta G \ll 0$, the reaction rate constant is insensitive to ΔG. In such a case, the activation energy is zero, and the rate constant is equal to the preexponent, k_H^0, in eq 4. Pines et al.[38] found that even the fastest proton transfer reactions are relatively slow, $\tau_D^{-1} < k_0 < \tau_S^{-1}$. Thus, dielectric relaxation provides the time clock for the proton transfer to the solvent reaction and not the fast solvation components, which are in the time-domain of tens of femtoseconds.[40] Thus, the main experimental findings of the proton-transfer experiments at low temperatures that the solvent characteristic time for the proton transfer is close to τ_D is in accordance with the findings of the proton-transfer structure reactivity relation.

Figure 3, parts a, b, and c, shows the experimental rate constant of DCN2 in the liquids used in this, and the previous study,[22] as a function of $1/T$ along with the computer simulation using the overall proton-transfer rate expression given by eq 3. As seen from the figure, the model calculation is in agreement with the DCN2 measurements. The model accounts for the low and the high-temperature regime as well as the intermediate regime between them. The parameters for the fit of Figure 3 are given in Table 1. There are three adjustable free parameters in the computer fits shown in Figure 3. These parameters are b, k_H^0 and $\Delta G_0^{\neq}$, where b is an empirical factor determined by $k_S(T) = b/\tau_D$, k_H^0 is the preexponential in eq 4 and $\Delta G_0^{\neq}$ is the intrinsic activation energy. For methanol, the parameters are as follows: $k_H^0 = 3 \times 10^{10}$ s^{-1} and $k_S(T) = 2.1/\tau_D$. From Table 1, we find that the preexponential k_H^0 is solvent dependent, and its value is similar to $1/\tau_D$ at room temperature and b ranges from 0.65 to 4. We used $\Delta G_0^{\neq} = 3$ kJ/mol for all three solvents. This value is slightly smaller than the one used by Pines et al.[38] The activation energies are only slightly dependent on the solvent and were calculated according to the Agmon−Levine structure reactivity relation. For methanol, the activation energy is $\Delta G^{\neq} = 2.1$ kJ/mol and $pK^*_{a,chem} = -0.37$.

From the model, it appears that, at low temperatures, a solvent motion with a characteristic time approximately that of the dielectric relaxation time, controls the reaction rate of the proton transfer. This is clearly seen in the case of proton transfer from excited DCN2 to neat protic solvents like methanol, ethanol, propanol, 1,2 ethanediol, 1,4 butanediol, and glycerol. At the high-temperature limit, the solvent relaxation time is faster than the tunneling process and the overall rate constant is determined by the proton tunneling.

An extension of this stepwise model can be described by a two-dimensional Markovian reaction−diffusion model.[41,42] Using such a model will increase the effective proton transfer rate, especially in the intermediate temperature range, where $k_S \approx k_H$. From Figure 4 it can be seen that, for methanol in this range, the computer fit underestimates the experimental proton-transfer rate.

Qualitative Comparison of the Temperature Dependence of Proton Transfer with the Borgis−Hynes Theory. In this section, we will compare our previous qualitative model based on the experimental results with the Borgis−Hynes theory for the proton transfer, which uses the Landau−Zener curve-crossing formulizm.[19−21]

The reaction can be described schematically

$$A^*H\cdots S_B \rightarrow A^{-*}\cdots HS_B^+$$

The reactant is an intermolecular hydrogen-bonded complex between the photoacid, AH^*, and a solvent molecule, S_B, that serves as a base, characterized by a hydrogen bond to the photoacid and also to other solvent molecules. It was found that this hydrogen bond in protic solvents shifts the fluorescence band to the red by about 1000 cm^{-1}.[39] In water, this specific water molecule, S_B, has three hydrogen bonds to three water molecules. To form the product, $A\cdots HS_B^+$, in water, one hydrogen bond of S_B to a water molecule must break. Thus, relatively long-range reorganization of the hydrogen bond network takes place upon proton transfer to the solvent. This

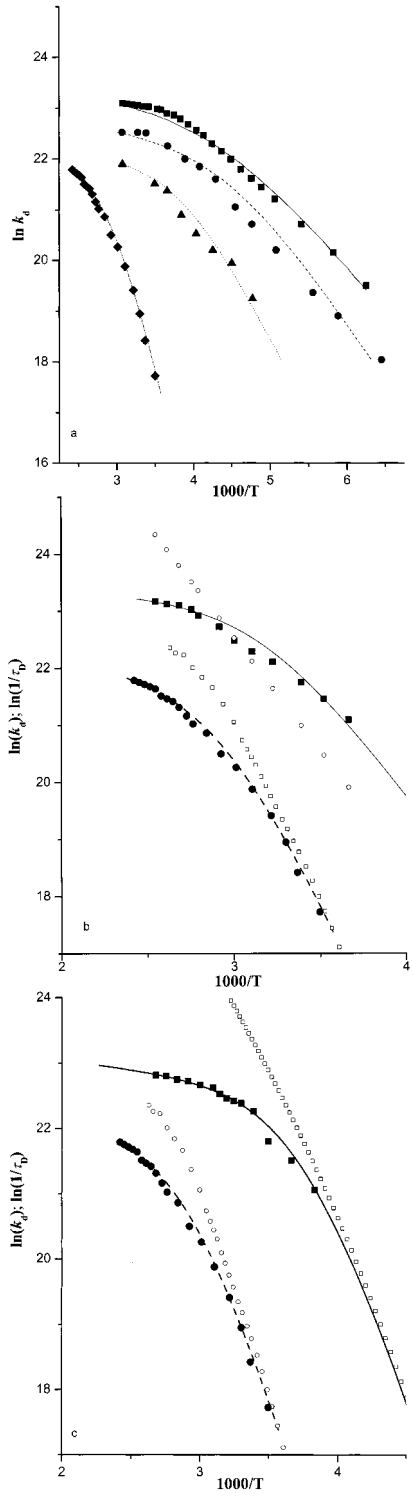

Figure 3. (a) Two step model calculations (see text) of the temperature dependence of the proton-transfer rate in methanol (solid line), ethanol (broken line), propanol (dotted line), and glycerol (dash−dot line), along with the experimental results—methanol (squares), ethanol (circles), propanol (triangles), and glycerol (diamonds). (b) Two step model calculations (see text) of the temperature dependence of the proton-transfer rate in 1,4-butanediol (solid line) and glycerol (dashed line), along with the experimental results—1,4-butanediol (squares) and glycerol (circles) and the dielectric relaxation time for 1,4-butanediol (open circles) and glycerol (open squares). (c) Two step model calculations (see text) of the temperature dependence of the proton-transfer rate in ethylene glycol (solid line) and glycerol (dashed line), along with the experimental results—ethylene glycol (circles) and glycerol (squares) and the dielectric relaxation time for ethylene glycol (open circles) and glycerol (open squares)

complex rearrangement, to accommodate the product, is probably the reason for a slow solvent generalized configuration motion, which corresponds to a low-frequency component in the solvent dielectric spectrum. Its time constant is close to the slow component of the dielectric relaxation time. According to Borgis and Hynes,[19] Bernstein and co-workers[11] and Syage,[13] a second important coordinate should be taken into account. This second coordinate is the distance between the two heavy atoms, O−H···O in our case. This distance is modulated by a low-frequency vibrational mode, Q.[11,19] The proton tunnels through the barrier from the reactant well to the product well via the assistance of the low frequency, Q, mode whenever the solvent configuration equalizes the energies of the reactant and the product. As mentioned above, our experiments indicate that the solvent fluctuation rate to equalize the energies is not of the order of 10^{13} s^{-1} but slower than 10^{12} s^{-1}. For monols, diols, and glycerol, it is very close to $1/\tau_D$, where τ_D is the slow component of the dielectric relaxation time.

Borgis and Hynes[19] derived an expression for the rate constant, k_{nm}, for a transition between the Q-vibrational state, n, in the reactant to the Q-vibrational state, m, in the product. They wrote an expression for k_{nm} in a transition state theory form. In particular, k_{nm} can be expressed as the average one-way flux in the solvent coordinate, through the crossing point S_{nm} of the two free energy curves for the n and m vibrational states, with the inclusion of the transmission coefficient, κ_{nm}^{wc}, giving the probability of a successful curve crossing

$$k_{nm} = \langle \dot{S}\, \Theta(\dot{S})\, \delta(S - S_{nm})\, \kappa_{nm}^{wc}(\dot{S}, S_{nm}) \rangle_R \qquad (6)$$

where S is the solvent coordinate, $\dot{S}$ is the solvent velocity, and $\Theta(\dot{S})$ is the positive velocity step function.

To find the appropriate nonadiabatic transmission coefficient factor, κ_{nm}^{wc}, for use in this equation, Borgis and Hynes[19] used the general Landau−Zener (LZ) transmission coefficient, κ_{nm}, adapted for the present problem. The LZ factor, appropriate for a positive velocity approach to the crossing point, is

$$\kappa_{nm} = [1 - {}^1/_2\exp(-\gamma_{nm})]^{-1}[1 - \exp(-\gamma_{nm})] \qquad (7)$$

$$\gamma_{nm} = \frac{2\pi C_{nm}{}^2}{\hbar(\partial \Delta V_{nm}/\partial S)_{S_{nm}} \dot{S}} = \frac{2\pi C_{nm}{}^2}{\hbar k_S \dot{S}} \qquad (8)$$

where ΔV_{nm} is the gap $V_m - V_n$ and includes multiple pass effects on the transition probability. (Note that $\kappa_{nm} \rightarrow 1$ is the adiabatic limit). When $\gamma_{nm} \ll 1$, one obtains the nonadiabatic limit result

$$\kappa_{nm}^{wc} = 2\gamma_{nm} \qquad (9)$$

This leads to

$$k_{nm} = \frac{2\pi}{\hbar} C_{nm}{}^2 \left[\left(\frac{\beta}{4E_S\pi}\right)^{1/2} e^{-\beta \Delta G_{nm}^{\neq}}\right] \qquad (10)$$

in which $\Delta G_{nm}^{\neq}$ is the activation free energy

$$\Delta G_{nm}^{\neq} = \frac{1}{4E_S}(E_S + \Delta G + \Delta E_{nm})^2 \qquad (11)$$

γ_{nm} (See eq 8) depends on the potential surfaces curvature, $(\partial \Delta V_{nm}/\partial S)_{S_{nm}}$, on $C_{nm}{}^2$ and on $\dot{S}$. $C_{nm}{}^2$ depends on the Q intermolecular vibrational mode which is independent of T and S. The solvent velocity, $\dot{S}$, strongly depends on the temperature.

TABLE 1: Relevant Parameters for Model Calculations

	$K^*_{a,chem}$	$pK^*_{a,chem}$	$\Delta G^{\neq}$ [kJ/mol]	$G_0^{\neq}$ [kJ/mol]	k_H^0 at 298 K [s^{-1}] 10^{-10}	k_H at 298 K [s^{-1}] 10^{-10}	k_S at 298 K [s^{-1}] 10^{-10}	τ_D[ps] at 298 K	b
MeOH	2.3	−0.37	2.0	3.0	2.9	1.25	4.3	48	2.1
EtOH	2.1	−0.33	2.1	3.0	1.5	0.63	1.7	132	2.3
Propanol	2.1	−0.33	2.2	3.0	0.80	0.33	1.2	341	4.0
Ethylene Glycol	2.3	−0.37	2.0	3.0	1.70	0.73	1.39	65	0.90
1,4-Butane Diol	2.6	−0.41	1.98	3.0	2.3	1.03	0.51	666	3.4
Glycerol	1.2	−0.08	2.8	3.0	0.90	0.21	0.011	5750	0.65

[a] pK^* is calculated by eq 5. The estimated error in the determination of pK^* is 8%. [b] b is an empirical factor used in the determination of the proton-transfer rate at the low-temperature range ($k_S(T) = (b)/(\tau_D)$, see text).

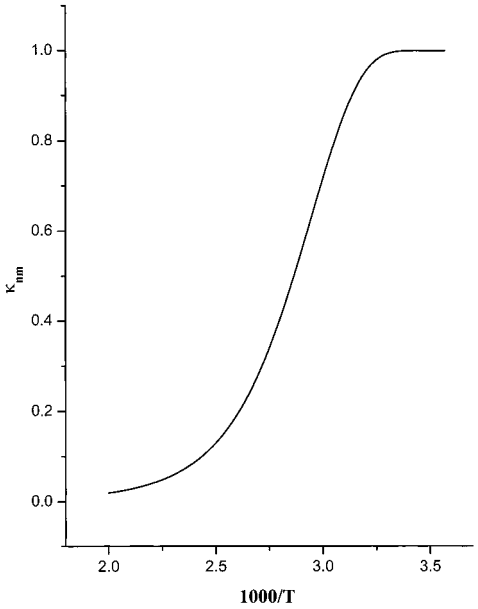

Figure 4. Landau−Zener (LZ) transmission coefficient κ_{nm} as a function of the temperature.

In fact, $\dot{S}$ relates to the solvent relaxation. On the basis of the experimental data, we infer that $\dot{S} = b/\tau_D$, where τ_D is the solvent dielectric relaxation time and b is a factor between 0.65 and 4. In all the solvents used, τ_D depends, nearly exponentially, on the temperature. The activation energy of τ_D of these solvents ranges from 12 kJ/mol (methanol) to 48 kJ/mol (glycerol). Thus, for glycerol and diols τ_D, changes by about 4 orders of magnitude within the temperature range studied, $\Delta T \cong 120$ K.

$$\gamma_{nm} \propto \tau_D(T);$$

$$\tau_D = \tau_D^0 \, e^{E_a/RT} \tag{12}$$

γ_{nm} assumes a low value at high temperature and a high value at low temperature. For the solvents used in this experiment, the value of γ_{nm} as a function of the temperature smoothly increases from a value close to 0, i.e., $\gamma \ll 1$ (the nonadiabatic limit) to a value $\gamma \gg 1$ (the adiabatic limit). An illustration of the temperature dependence of the transmission coefficient, κ_{nm}, for glycerol as solvent is shown in Figure 4. We used eqs 7 and 8 and $(2\pi C_{nm}^2)/(\hbar k_s) = 10^8$. τ_D is taken from Ref 31. It is clearly seen that the transmission coefficient, κ_{nm}, changes from close to zero at high temperatures (above 400 K) to close to 1 at low temperatures (below 325 K).

Borgis and Hynes[19] have also theoretically examined the situation of the adiabatic limit, which leads to the rate expression

$$k_{AD} = (\omega_s/2\pi) \exp(-\beta \Delta G^{\neq}) \tag{13}$$

where ω_S is the solvent frequency, and $\Delta G^{\neq}$ is the free energy of activation. In regular theoretical considerations, C_{nm}^2 is large, the gap is large, $\kappa_{nm} \approx 1$, and the reaction rate proceeds on an adiabatic potential surface. In our approach, C_{nm}^2 is an unknown, and approximately constant over the studied temperature range, but $\dot{S}$, the solvent velocity, appearing in the denominator of γ (eq 8) depends exponentially on the temperature. Thus, at slow solvent velocity $\gamma \gg 1$ and $\kappa_{nm} \approx 1$, the proton-transfer reaction proceeds adiabatically, that is, the rate-limiting step is the solvent velocity. According to Borgis and Hynes[19] (eq 13), the pre-exponential-factor will be of the order of 10^{13} s^{-1} or greater. This expression sets a limit of the fastest proton-transfer rate of about $(100\ fs)^{-1}$. Such a high rate was found so far only in intramolecular proton transfer.[43] This rate is almost larger by a factor of 100 than that of the one found experimentally for the fastest intermolecular proton transfer.

Rips and Jortner[44] derived an expression for the electron transfer (ET) rate, which bridges between the nonadiabatic and the solvent controlled adiabatic limit. They established simple criteria for the validity range of various descriptions of the ET dynamics, i.e., the transition state theory, the solvent controlled ET, and the adiabatic and nonadiabatic limits. The expression for the overall ET rate constant they derived is

$$k_{ET}^{-1} = (k_{ET}^{NA})^{-1} + (k_{ET}^{AD})^{-1} = \tau_{ET}^{AD} + \tau_{ET}^{NA} \tag{14a}$$

$$k_{ET} = \frac{k_{ET}^{NA} \, k_{ET}^{AD}}{k_{ET}^{NA} + k_{ET}^{AD}} \tag{14b}$$

where k_{ET}^{AD} and k_{ET}^{NA} are the adiabatic and nonadiabatic rate constants, respectively. These rate constants have a similar functional form to the proton-transfer rates given by Borgis and Hynes.[19]

Our previous stepwise model[22] is similar to the expression of Rips and Jortner[44] for the overall ET rate constant that bridges between the two extreme cases—the nonadiabatic and the adiabatic ET.

In this study, we propose to adopt qualitatively the Borgis−Hynes[19] formulas for nonadiabatic and adiabatic proton-transfer rate constants. These rates are used in a similar form as suggested by Rips and Jortner[44] for the overall expression of the electron-transfer rate constant (eq 14). To use the rate constants quantitatively, we face some unknown parameters. The rate constant for the nonadiabatic proton-transfer includes the unknown coupling matrix C. In the high-temperature regime, $\beta\hbar\omega_Q \ll 1$, the nonadiabatic reaction rate constant, when the reaction asymmetry magnitudes $|\Delta G| < E_S$, is

$$k = \frac{\beta \langle C^2 \rangle}{\hbar} \left(\frac{\pi}{\beta E_{tot}} \right)^{1/2} \exp(-\beta \Delta G^{\neq}) \tag{15}$$

where $E_{tot} = E_S + E_Q + E_\alpha$, and the thermally average square coupling is approximately

$$\langle C^2 \rangle \approx C_0 \exp\left[\frac{E_\alpha}{\hbar\omega_Q}\left(\frac{4}{\beta\hbar\omega_Q} + \frac{\beta\hbar\omega_Q}{3}\right)\right] \qquad (16)$$

Experimentally, in the high-temperature regimes, we find for DCN2, a super photoacid, very small activation energies, $\Delta G^{\neq}$ (see Figure 3). In addition, the apparent non-Arrhenius temperature behavior arising from the average square coupling, $\langle C^2 \rangle$ (eq 16), is, in practice, quite weak for typically realistic parameter values so that, for all practical purposes, k displays Arrhenius behavior, despite the fact that the intrinsic reactive event is quantum proton tunneling.[19] Because we do not know the coupling matrix element we can use the classical Arrhenius expression for the temperature dependence of the nonadiabatic rate constant

$$k_{PT}^{NA} = k_0 \exp(-\beta \Delta G_{NA}^{\neq}) \qquad (17)$$

For the adiabatic limit, Borgis and Hynes found[19] that

$$k_{PT}^{AD} = \left(\frac{\omega_S}{2\pi}\right) \exp(-\beta \Delta G_{AD}^{\neq}) \qquad (18)$$

for the symmetric case $\Delta G = 0$, $\Delta G_{AD}^{\neq} = \Delta G_{NA}^{\neq} - C_0$. Because $\Delta G_{NA}^{\neq}$ was found, experimentally, to be small, $\Delta G_{AD}^{\neq}$ is also very small. The prefactor, $(\omega_S)/(2\pi)$, is the solvent response frequency. Although Borgis and Hynes estimated that $\omega_S \approx 10^{13} s^{-1}$, our experimental findings relate the solvent response τ_S^{-1} to $\tau_L < \tau_S < \tau_D$ for the protic solvents we used. This slow response arises from the long-range solvent rearrangement needed to get to the crossing point in the curve crossing formulation. To equalize the energies of the reactant and products, the hydrogen bond network of both the reactant and product needs a large change. The characteristic time, τ_S, for this change is probably long. Evidence for such long times is given by the structure reactivity (free energy relation) of proton-transfer reactions.

We propose to use a similar expression to the one used by Rips and Jortner[44] that bridges between the nonadiabatic and the solvent controlled adiabatic limit (eq 14). For the proton transfer to the solvent

$$k_{PT}(T) = \frac{k_{PT}^{NA}(T) k_{PT}^{AD}(T)}{k_{PT}^{NA}(T) + k_{PT}^{AD}(T)} \qquad (19)$$

The formal expressions for k_{PT}^{NA} and k_{PT}^{AD} are given by eqs 17 and 18. k_{PT}^{NA} is qualitatively parallel to k_H in eq 3. Accordingly, the prefactor, k_H^0, depends on the thermally average square coupling matrix (eq 16). k_{PT}^{AD} is similar to k_S in eq 3. The time scale of the solvent control is slow and is close to τ_D. Using eq 19 to calculate $k_{PT}(T)$ as a function of the temperature results in a qualitatively similar behavior to eq 3. Figure 3 shows such a fit to the experimental data. As can be seen, the fit is good for all solvents shown. These solvents differ in their characteristic dielectric relaxation time by a factor of 100. The lowest temperature is 160 K for methanol and ethanol, and the highest temperature is 410 K for the diols and glycerol.

Summary

We have studied by time-resolved emission techniques the proton dissociation and the reversible geminate recombination processes in alcohols. DCN2 was used as the excited-state proton emitter (photoacid). The experimental time-resolved fluorescence data were analyzed by the exact numerical solution of the transient Debye−Smoluchowski equation (DSE).

We have found that the proton dissociation rate constant, k_d, of excited DCN2 in neat monols, diols, and glycerol at relatively high temperatures is almost temperature independent, whereas at lower temperatures, the proton-transfer rate is similar to the inverse of the dielectric relaxation time.

We used the Borgis−Hynes proton transfer theory based on the Landau−Zener curve crossing formulation to fit qualitatively the experimental results. The results show that the unusual temperature dependence of proton transfer to the solvent can be explained as a continuous transition from the nonadiabatic regime (the high-temperature limit) to the adiabatic regime (the low-temperature limit).

Acknowledgment. We thank Prof. L. Tolbert for providing the 5,8-dicyano-2-naphthol. D.H. would like to thank Prof. M. Bixon and Prof. I. Rips for helpful discussion. This work was supported by grants from the Israel Science Foundation and the James-Franck German-Israel Program in Laser-Matter Interaction.

References and Notes

(1) Ireland, J. F.; Wyatt, P. A. H. *Adv. Phys. Org. Chem.* **1976**, *12*, 131.

(2) Huppert, D.; Gutman, M.; Kaufmann, K. J. In *Advances in Chemical Physics*; Jortner, J., Levine, R. D., Rice, S. A., Eds.; Wiley: New York, 1981; Vol. 47, 681. Koswer, E.; Huppert, D. In *Annual Reviews of Physical Chemistry*; Strauss, H. L.; Babcok, G. T., Moore, C. B., Eds.; Annual Reviews Inc: 1986; Vol. 37, 122.

(3) Lee, J.; Robinson, G. W.; Webb, S. P.; Philips, L. A.; Clark, J. H. *J. Am. Chem. Soc.* **1986**, *108*, 6538.

(4) Gutman, M.; Nachliel, E. *Biochim. Biophys. Acta* **1990**, *391*, 1015.

(5) Förster, T. *Z. Natuwissenschaft* **1949**, *36*, 186.

(6) Weller, A. *Progress Reaction Kinetics* **1961**, *1*, 189.

(7) Kolodny, E.; Huppert, D. *J. Chem. Phys.* **1981**, *63*, 401.

(8) Ando, K.; Hynes, J. T. In *Structure, Energetics and Reactivity in Aqueous Solution*; Cramer, C. J., Truhlar, D. G., Eds.; ACS Books: Washington, DC, 1994.

(9) Agmon, N.; Huppert, D.; Masad, A.; Pines, E. *J. Phys. Chem.* **1991**, *96*, 952.

(10) Knochenmuss, R. *Chem. Phys. Lett.* **1998**, *293*, 191.

(11) Hineman, M. F.; Brucker, G. A.; Kelley, D. F.; Bernstein, E. R. *J. Chem. Phys.* **1992**, *97*, 3341.

(12) Peters, K. S.; Cashin, A.; Timbers, P. *J. Am. Chem. Soc.* **2000**, *122*, 107.

(13) Syage, J. A. *J. Phys. Chem.* **1995**, *99*, 5772.

(14) Gandour, R. D.; Schowen, R. L. *Transition States of Biochemical Processes*; Plenum: New York, 1978.

(15) Bell, R. P. *The Tunnel Effect in Chemistry*; Chapman and Hall; London, 1980.

(16) Westheimer, F. H. *Chem. Rev.* **1961**, *61*, 265.

(17) Bell, R. P. *The Proton in Chemistry*; Cornell University Press: Ithaca, 1973.

(18) German, E. D.; Kuznetsov, A. M.; Dogonadze, R. R. J. *Chem. Soc., Faraday Trans. 2* **1980**, *76*, 1128. Ulstrup, J. *Charge-Transfer Processes in Condensed Media*; Springer: Berlin, 1979.

(19) Borgis, D.; Hynes, J. T. *J. Phys. Chem.* **1996**, *100*, 1118. Borgis, D. C.; Lee, S.; Hynes, J. T. *Chem. Phys. Lett.* **1989**, *162*, 19. Borgis, D.; Hynes, J. T. *J. Chem. Phys.* **1991**, *94*, 3619.

(20) Cukier, R. I.; Morillo, M. *J. Chem. Phys.* **1989**, *91*, 857. Morillo, M.; Cukier, R. I. *J. Chem. Phys.* **1990**, *92*, 4833.

(21) Li, D.; Voth, G. A. *J. Phys. Chem.* **1991**, *95*, 10 425. Lobaugh, J.; Voth, G. A. *J. Chem. Phys.* **1994**, *100*, 3039.

(22) Cohen, B.; Huppert, D. *J. Phys. Chem. A* **2000**, *104*, 2663.

(23) Tolbert, L. M.; Haubrich, J. E. *J. Am. Chem. Soc.* **1990**, *112*, 8163. Tolbert, L. M.; Haubrich, J. E. *J. Am. Chem. Soc.* **1994**, *116*, 10 593.

(24) Pines, E.; Huppert, D.; Agmon, N. *J. Chem. Phys.* **1988**, *88*, 5620.

(25) Agmon, N.; Pines, E.; Huppert, D. *J. Chem. Phys.* **1988**, *88*, 5631.

(26) Debye, P. *Trans. Electrochem. Soc.* **1942**, *82*, 265.

(27) Carmeli, I.; Huppert, D.; Tolbert, L. M.; Haubrich, J. E. *Chem. Phys. Lett.* **1996**, *260*, 109

(28) Erdey-Gruz, T.; Lengyel, S. In *Modern Aspects of Electrochemistry*; Bockris, J. O'M., Conway, B. E., Eds.; Plenum: New York, 1964; Vol. 12, pp 1−40.

(29) Dolgin, B. MSc Thesis, Ben-Gurion University, Beer Sheva, 1997.
(30) Landolt-Bornstein, Vol.*2*, Part 5a: Andrussow, L.; Schramm, B. Eds.; K. Schaffer, Springer, Berlin, 1969.
(31) Richert, R. unpublished results; Bötcher, C. J. F.; Bordevik, P. *Theory of Electric Polarization*; Elsevier, Amsterdam, 1978; Vol. II, p 254.
(32) Bertolini, D.; Cassettari, M.; Salvetti, G. *J. Chem. Phys.* **1983**, *78*, 365.
(33) Garg, S. K.; Smyth, C. P. *J. Phys. Chem.* **1965**, *69*, 1294.
(34) Agmon, N.; Goldberg, S. Y.; Huppert, D. *J. Molecular Liquids* **1995**, *64*, 161.
(35) Kreevoy, M. M.; Kotchevar, A. T. *J. Am. Chem. Soc*. **1990**, *112*, 3579; Kotchevar, A. T.; Kreevoy, M. M. *J. Phys. Chem.* **1991**, *95*, 10 345.
(36) Poles, E.; Cohen, B.; Huppert, D. *Israel J of Chem* **1999**, *39*: (3−4) 347.
(37) Agmon, N.; Levine, R. D. *Chem. Phys. Lett.* **1977**, *52*, 197. Agmon, N.; Levine, R. D. *Israel J. Chem.* **1980**, *19*, 330.
(38) Pines, E.; Fleming, G. R. *Chem. Phys. Lett*. **1994**, *183*, 393. Pines, E.; Magnes, B.; Lang, M. J.; Fleming, G. R. *Chem. Phys. Lett.* **1997**, *281*, 413.
(39) Solntsev, K.; Huppert, D.; Agmon, N. *J. Phys. Chem. A* **1999**, *103*, 6984.
(40) Jimenez, R.; Fleming, G. R.; Kumar, P. V.; Maroncelli, M. *Nature* **1994**, *309*, 471.
(41) Agmon, N.; Rabinovich, S. *J. Phys. Chem.* **1992**, *97*, 7270.
(42) Bicout, D. J.; Szabo, A. *J. Chem. Phys.* **1998**, *109*, 2325.
(43) Chudoba, C.; Riedle, E.; Pfeiffer, M.; Elsaesser, T. *Chem. Phys. Lett.* **1996**, *263*, 622.
(44) Rips, I.; Jortner, J. *J. Chem. Phys.* **1987**, *87*, 2090.